

**CHEMICAL COMPOSITION AND IRON OXIDATION STATE OF THE AMORPHOUS SILICATE MATRIX IN ACFER 094.** T. Hopp<sup>1,2</sup>, C. Vollmer<sup>2</sup>, D. Lautenschläger<sup>2</sup>, M. Pelka<sup>2</sup> and J. Render<sup>1,2</sup>, <sup>1</sup>Universität Münster, Institut für Planetologie, Germany, timo.hopp@wwu.de; <sup>2</sup>Universität Münster, Institut für Mineralogie, Germany.

**Introduction:** The unique ungrouped carbonaceous chondrite Acfer 094 is to date one of the most pristine meteorites available for study. The major component in this primitive chondrite is the fine-grained matrix (grain size  $\ll 10 \mu\text{m}$ ). This matrix consists of an unequilibrated mixture of anhydrous silicates, sulfides, metal grains, and amorphous silicate material [1]. This amorphous silicate material is the major component of the fine-grained matrix and indicates very low thermal and aqueous alteration effects, which would have led to recrystallization of the amorphous material. Furthermore, the high reactivity of this amorphous phase makes it a sensitive indicator for small-scale aqueous alteration effects, which cannot be observed in bulk sample analysis.

The origin of the amorphous silicate matrix is not yet clear. The main scenarios include either primary processes before accretion of the parent body, e.g. disequilibrium condensation from a fractionated solar gas, or secondary processes on the parent body, e.g. aqueous alteration of a precursor material [1]. Linking changes in the chemical composition and the oxidation states of Fe in the amorphous silicate matrix to petrographic observations could reveal information about alteration effects and possible formation scenarios of amorphous silicate matrix. Here we report on analytical transmission electron microscopy (TEM) investigations of six electron-transparent Acfer 094 matrix samples to put constraints onto these issues.

**Samples and methods:** The six TEM lamellae of the amorphous silicate matrix in Acfer 094 have been prepared from a polished thin-section using focused ion beam techniques (FIB) for previous investigations on presolar grains in the matrix [2]. The chemical compositions in the three samples 3113, 2520, and 2106 were determined using a Jeol JEM-3010 TEM (300 kV) with an Oxford Isis EDX system. Experimentally determined and published Cliff-Lorimer-k-factors were used to measure the chemical composition of 25 to 30 spots in each of the three samples [3].

The oxidation states of Fe in the six samples were measured using a Zeiss Libra 200FE TEM (200 kV) with an in-column  $\Omega$ -energy filter for Electron Energy Loss Spectroscopy (EELS). For each sample, 14 EEL spectra at the Fe-L<sub>23</sub> edge were acquired at different sample regions to improve the reproducibility and accuracy. The Fe<sup>3+</sup>/ΣFe ratios were calculated using the modified integral intensity ratio technique [4]. In both approaches, the amorphous areas in the samples were carefully

selected using the TEM diffraction mode prior to EDX/EELS analyses to exclude contribution from crystalline grains, i.e., silicates or nanosulfides. The texture of each sample was also examined by Z-contrast imaging (high angle annular darkfield, HAADF) in scanning TEM mode.

**Results:** Mineralogical and textural differences in the samples can be observed on a sub- $\mu\text{m}$  scale (Fig. 1). The amount of sulfide and metal grains vary in the samples. Moreover, differences in the porosity of the samples are visible. The sample 3113 represents an unequilibrated mineral assemblage with widespread porosity (Fig. 1B). In contrast, sample 2106 has nearly no porosity and very low amounts of sulfide and metal grains. Within the amorphous matrix of 2106 small bright veins indicate secondary recrystallization effects (Fig. 1A).

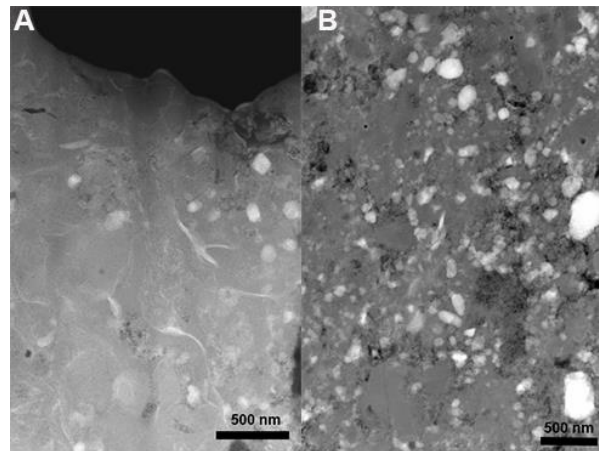
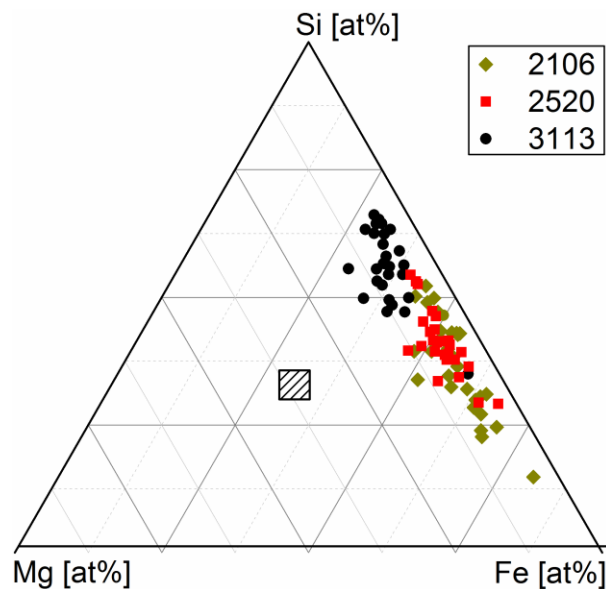


Figure 1: STEM-HAADF micrographs of samples 2106(A) and 3113(B).

The EDX results display inhomogeneities in the Fe/Si, Ca/Si, and S/Si ratios of the three samples. Compared to published values [1] the generally low and invariable Mg/Si ratios in contrast to variable Fe/Si ratios stand out (Fig. 2). Compared to the solar abundances, the results show a high depletion in Mg and S in the amorphous matrix.

The results of the EELS analyses are summarized in Fig. 3. All six investigated samples show a generally high oxidation state with the lowest Fe<sup>3+</sup>/ΣFe of 0.66(0.02) in sample 3113. With increasing oxidation state of Fe, the range of the Fe<sup>3+</sup>/ΣFe ratios within the samples also slightly increases as indicated as well by a higher standard deviation. The sample 2106 has the

highest  $\text{Fe}^{3+}/\Sigma\text{Fe}$  of 0.73(0.03). Compared to published values of 50% to 90%  $\text{Fe}^{3+}$  contents for Acfer 094 matrix [6], our results are clearly more homogeneous.



**Figure 2:** Mg-Si-Fe ternary diagram plots the analyzed spot analyses of the three samples. The patterned square displays the solar composition [5].

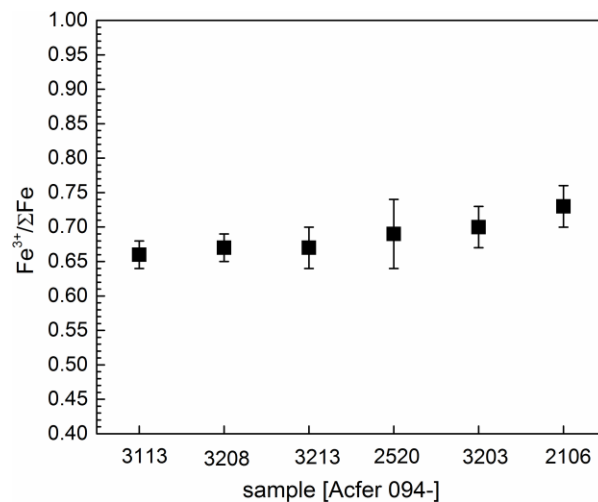


**Figure 3:** Oxidation state of Fe for six samples of the amorphous silicate matrix in Acfer 094. Each square represents the mean value of 14 EEL spectra of the respective sample with the standard deviation ( $1\sigma$ ).

**Discussion:** The textural differences of the samples can be explained by subtle aqueous alteration processes on the parent body. Interaction with aqueous fluids led to crystallization of hydrous phyllosilicates, which

fill up the porosity, and enhances oxidation of the metal and sulfide grains. The EDX and EELS analyses of the six samples also reveal nm-scale compositional differences in the amorphous silicate matrix. This chemical inhomogeneity supports the textural evidences of aqueous alteration effects. Aqueous alteration preferentially mobilizes Fe. Hence, the Fe/Si ratios increase with proceeding aqueous alteration. The high depletion and invariable Mg/Si ratios on the other hand could be remnants of the formation process, e.g., fractional disequilibrium condensation from a Mg-depleted gas, which is similarly proposed for the formation of GEMS grains [7].

The homogeneous high oxidation state of Fe in the amorphous silicate matrix could reveal information of a possible formation scenario. In case of disequilibrium condensation in the solar nebula, the amorphous silicate matrix would be a primary phase, and should record the generally reducing conditions of the early solar nebula. A formation due to parent body alteration, on the other hand, should have led to major inhomogeneities of the oxidation state as in other, more altered CR and CM chondrites [8], which we do not observe. We therefore favor a scenario in which a Mg-depleted nebular precursor material, must have been homogeneously oxidized prior to accretion of the Acfer 094 parent body, probably due to reactions with water vapor. Acfer 094 apparently formed in a reservoir favorable for such nebular oxidation as also indicated by cosmic symplectite (COS) in its matrix [9].

**Conclusion:** The amorphous silicate matrix in Acfer 094 has nm-scale differences in the composition and the oxidation state of Fe. These subtle heterogeneities can be best explained by small-scale aqueous alteration processes on the parent body. However, the generally high oxidation state and invariable Mg-depleted compositions could indicate formation of the amorphous silicate matrix as a nebular oxidation product of a fractionated solar gas component.

**References:** [1] Greshake A. (1997) *Geochim. Cosmochim. Acta*, 57, 1521-1550. [2] Vollmer C. et al. (2009) *Geochim. Cosmochim. Acta*, 73, 7127-7149. [3] Cliff G. and Lorimer G. W. (1975) *J. Microsc.*, 103, 203-207. [4] van Aken P. A. and Liebscher B. (2002) *Phys. Chem. Miner.*, 29, 188-200. [5] Lodders K. et al. (2009) In *Landolt-Börnstein, New Series*, 4, 560-630. [6] Keller L. P. and Messenger S. (2012) *LPS XXXXIII*, Abstract #1880. [7] Keller L. P. and Messenger S. (2011) *Geochim. Cosmochim. Acta*, 75, 5336-5365. [8] Le Guillou et al. (2014) *LPS XXXXV*, Abstract #2052. [9] Seto Y. et al. (2009) *Geochim. Cosmochim. Acta*, 72, 2723-2734.